Thin Films of Functionalized Multiwalled Carbon Nanotubes as Suitable Scaffold Materials for Stem Cells Proliferation and Bone Formation

Tapas R. Nayak,[†] Li Jian,[†] Lee C. Phua,[†] Han K. Ho,[†] Yupeng Ren,[‡] and Giorgia Pastorin[†,*]

[†]Department of Pharmacy, National University of Singapore, Block S15#05-PI-03, Singapore 117543 and [‡]Shanghai Institute of Materia Medica, Chinese Academy of Sciences, 555 Zu Chong Zhi Road, Shanghai, 201203, China

ABSTRACT In the field of regenerative medicine, human mesenchymal stem cells envisage extremely promising applications, due to their ability to differentiate into a wide range of connective tissue species on the basis of the substrate on which they grow. For the first time ever reported, we investigated the effects of a thin film of pegylated multiwalled carbon nanotubes spray dried onto preheated coverslips in terms of their ability to influence human mesenchymal stem cells' proliferation, morphology, and final differentiation into osteoblasts. Results clearly indicated that the homogeneous layer of functionalized nanotubes did not show any cytotoxicity and accelerated cell differentiation to a higher extent than carboxylated nanotubes or uncoated coverslips, by creating a more viable microenvironment for stem cells. Interestingly, cell differentiation occurred even in the absence of additional biochemical inducing agents, as evidenced by multiple independent criteria at the transcriptional, protein expression, and functional levels. Taken together, these findings suggest that functionalized carbon nanotubes represent a suitable scaffold toward a very selective differentiation into bone.

KEYWORDS: mesenchymal stem cells · carbon nanotubes · functionalization · cell differentiation · bone · osteogenesis.

The ambitious goal in the design of biomimetic materials for application to tissue engineering and repair is to create biocompatible scaffolds with suitable physical and chemical properties and to guarantee proper adhesion and sustained cell growth. These biomaterials may provide functional substitutes of native tissues to serve not only as grafts for implantation[1] but also as physiologically relevant models for controlled studies of cell function and bone development.[2] However, the identification of materials capable of promoting the desired cellular and tissue behavior is still a major challenge facing the field of tissue engineering. To alleviate this problem, engineers and clinicians alike have been pursuing the development of hybrid or composite biomaterials to synergize the beneficial properties of multiple materials in a superior matrix.

Recently, carbon nanotubes (CNTs) have emerged as a promising material for such purposes, due to their tremendous strength, ultralight weight, and high stability and their ability to become very flexible after suitable functionalization (f-CNTs).[3,4] On the other hand, modern tissue engineering strategies tend to combine these scaffold materials with living cells to develop biological substitutes that can restore tissue functions.[5−7] Since tissue specific cell types are not always available in sufficient amounts to guarantee complete recovery of damaged tissue, stem cells embody a striking alternative for tissue engineering. More precisely, adult stem cells, such as human mesenchymal stem cells (hMSCs), are considered the most promising multipotent species, since they have a high-differentiation potential into diversified lineages without being tumorigenic.[8]

Until now, the combination of CNTs and hMSCs has been very ineffective, primarily because of CNTs' impurities (mainly catalysts and amorphous carbon) deriving from their production and remaining even after some purification processes.[9] These contaminations are often responsible for cytotoxic effects and have thus hindered the extensive use of this material for any biomedical application. In addition, one severe limitation is the difficulty in creating a uniform microenvironment for proper cell growth with carbon nanotubes of variable lengths. Only very recently, conductive CNTs have been found to support neuronal cell growth (although not necessarily differentiation from their progenitor cells), thus providing new insights for the application of this material as a scaffold for prostheses.[10−12] Here we explore the ability of a homogeneous thin film formed by

*Address correspondence to phapg@nus.edu.sg.

Received for review October 13, 2010 and accepted November 18, 2010.

Published online November 30, 2010.
10.1021/nn102738c

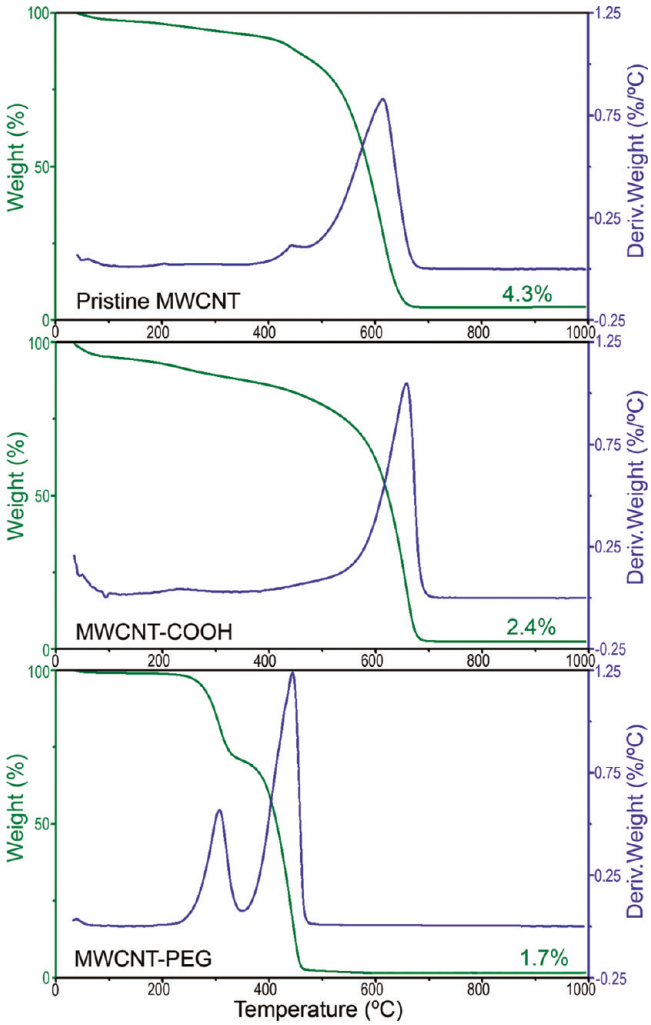

Figure 1. TGA graphs and derivative curves of MWCNT samples. TGA graphs are labeled with the wt % of metal residue after ramping the sample to 1000 °C.

well-dispersed, functionalized multiwalled carbon nanotubes (f-MWCNTs) sprayed onto plain coverslips to assist in the induction of hMSCs differentiation into osteogenic lineages, even in the absence of any biochemical inducer.

To that purpose, we selected and utilized polyethylene glycol-conjugated multiwalled carbon nanotubes (MWCNT-PEG) as a composite biomaterial to promote the osteogenic differentiation of hMSCs and simultaneous bone matrix mineralization. These functionalized CNTs (f-CNTs) were uniformly dispersed at a concentration of 10 mg/mL (as determined from previous dispersibility studies (Table S1 in Supporting Information) and sprayed onto preheated coverslips to get a uniform and smooth coating. We aimed to evaluate the suitability of this matrix for further development by objectively measuring its impact on cell viability as well as the inheritance of osteogenic phenotype.

Recent advances have shown that besides cell surface interactions, distinct nanopatterning of biomimetic surfaces[13,14] contributes significantly to cell behavior and differentiation.[15−17] More precisely, cell adhesion, spreading, proliferation, and differentiation seem to be influenced by the substrates on which stem cells grow. In this article we have shown for the first time that MWCNTs, once functionalized with hydrophilic PEG chains, become biocompatible scaffolds to support hMSCs' growth and proliferation, since they do not affect cell viability. Furthermore, we demonstrated that a compact and uniform thin film of tubes presenting some nanometric irregularities can provide a suitable environment to enable stem cells to differentiate into osteogenic lineage. Indeed we speculated that the combination of the mechanical properties of CNTs, together with the efficient differentiation of stem cells into bone, could pave the way toward the extensive use of this material for the regeneration of functional tissues.

RESULTS AND DISCUSSION

The first challenge in this work consisted of the surface modification to achieve biocompatible MWCNT materials. MWCNTs were functionalized following the procedure reported elsewhere,[18] and they were confirmed by thermogravimetric analysis (TGA) measurements (Figure 1). In agreement with the work performed by Zhao and collaborators,[18] the TGA graphs showed distinct derivative curves of pristine MWCNTs, oxidized nanotubes (MWCNT-COOH) and MWCNT-PEG complexes (MWCNT-PEG). The weight percentage of metal residue was 2.4% for MWCNT-COOH (990 °C) and 1.7% for MWCNT-PEG (990 °C). On the basis of these measurements, we estimated the loading of MWCNTs in MWCNT-PEG to be about 70.8%. From these graphs, the extent of PEG (MW 600) complexed with MWCNTs was determined to be [(100 − 70.8)/600]/ (70.8/12) = 0.8%.

Further characterization through transmission electron microscopy (Figure S1 in Supporting Information) showed that acidic treatment and sonication for 6 h shortened MWCNTs (lengths of oxidized MWCNT-COOH ranged between 400 and 800 nm) in comparison to pristine tubes, while their diameters remained intact. The additional presence of PEG helped in the formation of more uniform suspensions and resulted in a dispersed network of interconnected MWCNT-PEGs. An additional aspect to consider is that PEG, in form of hydrogel, was found to enhance cell viability of hMSCs,[19] and stem cells photoencapsulated with PEG hydrogels promoted homogeneous deposition of neocartilage when induced for chondrogenic differentiation.[20] Moreover optical images of f-CNTs sprayed onto coated coverslips presented some irregularities and uneven layers (*i.e.*, breaks of coverslips without CNTs) in the case of MWCNT-COOH, while they showed a full and compact film with MWCNT-PEG (Figure S3 in Supporting Information). Since it is known that surface regularity is an important factor in cell proliferation and

differentiation,[21,22] therefore these results predicted a better cell growth in case of MWCNT-PEGs.

Furthermore it has been previously shown that a certain type of topography, specifically the roughness of the underlying substrates (in our case CNT-PEG thin film), influences spatial distribution and cell differentiation,[23,24] since it affects the specific adsorption of proteins at the surface and the subsequent cell reactions. Therefore the atomic force microscopy (AFM) (Veeco dimension 3100, United States) measurements were taken to determine the roughness of coverslips coated with different f-CNTs (Figure 2).

Table 1 shows the analysis of the surface roughness of different coatings as determined by AFM. Although all coatings formed a rough surface, MWCNT-PEG thin films, with an average roughness of 18.3 nm, showed comparatively smoother surfaces than MWCNT-COOH coatings, with an average roughness of 41.4 nm. Likewise, peak-to-peak deviation of roughness was also higher for MWCNT-COOH-coated surfaces than the MWCNT-PEG-coated surfaces. Our results indicated that the roughness obtained in the coated samples consisted of nanometric irregularities in the form of either randomized (as in MWCNT-COOH, Figure 2a) or slightly parallel (as in MWCNT-PEG, Figure 2b) grooves and ridges. We hypothesized that these parallel grooves helped in the proper growth of stem cells over the whole period of incubation and eventually favored their further differentiation into bone lineage. In fact it has been shown that stem cells' fate can be selectively guided by regulating nanometric dimensions of the substrates,[25] although further investigations are required to fully understand the mechano-sensing phenomenon behind such observation.

The subsequent growth of human mesenchymal stem cells on different substrates was evaluated by incubating hMSCs onto f-MWCNT-coated coverslips. To prove that MWCNTs did not affect normal cell growth, our group has previously reported enhanced biocompatibility of these ultrapure MWCNTs,[26] where no cytotoxicity was observed until a concentration of 150 μg/mL in the cell culture medium. Unlike that study where breast cancer cells (MCF-7) were exposed to different nanotubes, including ultrapure MWCNTs, in this investigation we incubated hMSCs with ultrapure MWCNTs over periods of 24, 48, and 72 h. This change enables us to directly assess the effect on a clinically relevant cell type, as cell viability is likely to differ between cell lines of cancerous and noncancerous origin. As seen in Figure 3, the 3-(4,5-dimethylthiazol-2-yl)-2,5-diphenyltetrazolium bromide (MTT) assay of hMSCs did not reveal any cytotoxicity in the case of ultrapure MWCNTs at concentrations up to 100 μg/mL (Figure 3a) and incubation periods up to 72 h (Figure 3b); a statistically negligible difference ($p \sim 1$) was detected in such a range. To exclude the possibility that black carbon nanotubes interfered with the result of the MTT assay,

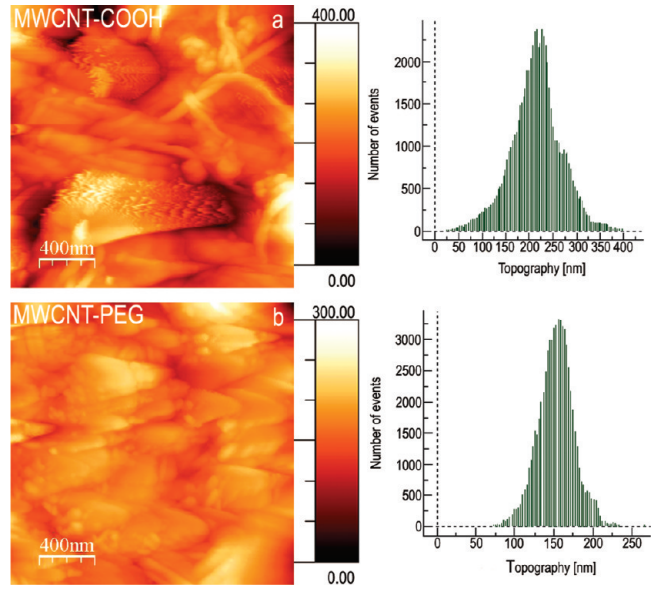

Figure 2. AFM images including the topography of the surfaces of MWCNT- and MWCNT-PEG-coated coverslips.

we also performed a CyQUANT assay of ultrapure MWCNTs for hMSCs at the same range of concentrations used for the above-reported MTT assays. As expected, the result was comparable to that of the MTT assay, as no cytotoxicity was observed until 100 μg/mL. Notably, although the concentration used in airbrushed MWCNTs (10 mg/mL) is much higher than the one tested for cytotoxicity assays, the thin films of nanotubes obtained in this study were expected to remain compact over the time, and only a minimal concentration (determined as equal or inferior to 10 μg/mL) would be released from the MWCNT-PEG thin film over the whole time of the experiments.

Moreover, these ultrapure tubes were pristine, not functionalized CNTs, which are known to display lower cell viability in comparison to f-CNTs. Therefore, we expected even better profiles with functionalized MWCNT-PEG samples; indeed this was confirmed by a calcein acetoxymethyl ester (AM) cell viability assay performed on all the samples following a previously reported procedure.[27] Images under a fluorescence microscope (Figure 4a−d) showed that cell morphology was, in general, similar across PEG alone, CNTs samples, and coverslips after 15 days of incubation in normal stem cell media. More precisely, stem cells grown on PEG alone (Figure 4b) and on MWCNT-PEG (Figure 4d) presented an elongated, fibroblast-like morphology comparable to those on coverslips (Figure

TABLE 1. AFM Data Showing Average, Root-Mean Square and Peak-to-Peak Deviation of Surface Roughness between Surfaces of Coverslips Coated with MWCNT-COOH and MWCNT-PEG

samples	average (nm)	rms (nm)	peak to peak (nm)
MWCNT-COOH	41.4	54.6	433
MWCNT-PEG	18.3	23.9	270

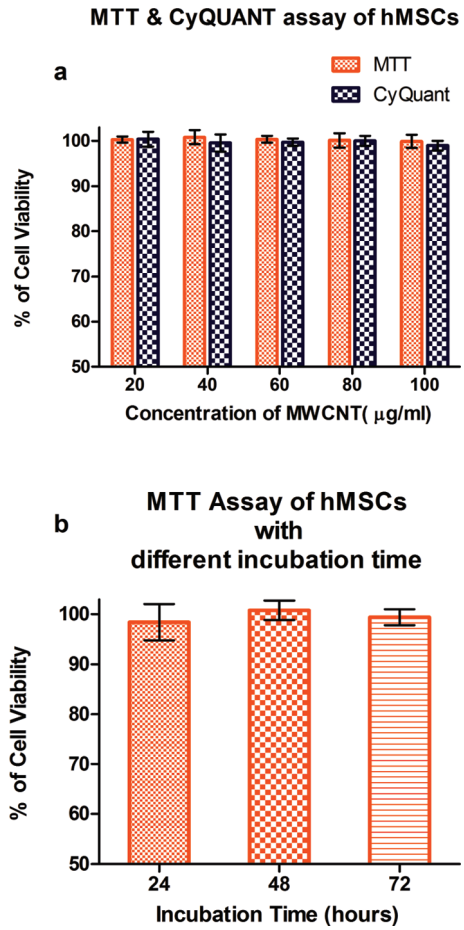

Figure 3. (A) Percentage of cell viability as obtained by MTT and CyQUANT assays of hMSCs after 24 h exposure to Ultrapure MWCNTs at the following concentrations: 20, 40, 60, 80, and 100 μg/mL ($p \sim 1$). (B) MTT assay at different time frames (24, 48, and 72 h) of hMSCs incubated at the highest dose (100 μg/mL.). No cytotoxicity was observed in the range of incubation time periods used for the purpose ($p \sim 1$).

4a), while in the case of MWCNT-COOH substrates, cells showed slightly irregular shapes, suggesting poor adherence to the substrate and thus lower cell growth (Figure 4c). To reiterate, cell viability in case of MWCNT-PEG-coated coverslips showed no significant difference ($p > 0.05$) when compared with cell viability on plain or only PEG-coated coverslips (Graph 4e). This is in agreement with some articles indicating that cytotoxicity is inversely correlated to the extent of CNTs' functionalization,[26,28,29] and it supports the promising role of these ultrapure, functionalized MWCNTs as biocompatible scaffolds. The only exception was represented by the MWCNT-COOH samples, for which cell viability was about 75%. This result conformed to the study performed by Liu *et al.*,[30] where cell proliferation and osteogenic differentiation of hMSCs were inhibited by carboxylated single-walled and MWCNTs.

Cell proliferation was confirmed by SEM imaging. Figure 4f clearly showed the distribution of hMSCs growing on a uniform substrate, while a zoomed area (Figure 4g) enabled the identification of a typical cell with its reticular fibrils on a homogeneous lattice of CNTs. In contrast, the growth of hMSCs on MWCNT-COOH-coated coverslips could not be visualized by SEM, as the coating was unstable during the process of critical point drying.

Furthermore, since a prerequisite for a successful implant is its stability over the time, additional samples of f-MWCNT coatings were shaken in Petri dishes containing distilled water using a Stuart gyro-rocker at 30 rpm for a time corresponding to the whole duration of the experiments. As expected, the MWCNT-COOH coating was destroyed within the first two hours of shaking, while the MWCNT-PEG coating remained intact for one week, after which it detached from the coverslip, but it did not undergo destruction (figure not shown). Due to the fact that in real implants these thin films would be embedded inside the damaged tissue rather than freely suspended in solution, this result suggests that the use of thin films made up of PEG-functionalized carbon nanotubes could provide a solid and stable structure for the growth of cells.

Although mesenchymal stem cells are known to represent a heterogeneous population of cells, in the present study we speculated that, once grown onto MWCNT-PEG substrates, they were capable of osteogenic differentiation. To substantiate such hypothesis, we characterized the transcriptional upregulation of osteopontin (OPN), an early biomarker for osteogenesis (Figure 5a)[31] in hMSCs grown onto different substrates and cultured for 14 days in osteogenic media with or without additional growth factor (*e.g.*, recombinant bone morphogenetic protein, BMP-2, at a concentration of 150 ng/mL). Expression changes in various samples were measured as fold change with respect to control cells (*i.e.*, positive control in form of hMSCs grown on coverslip in the presence of BMP-2 with osteoinduction media and negative control consisting of coverslips without BMP-2 and cultured in normal stem cell media). Reverse transcription polymerase chain reaction (RT-PCR) measurements showed that BMP-2 mediated greater than two-fold elevation of OPN expression for hMSCs grown on either coverslip or PEG-coated layer. Strikingly, MWCNT-PEG, even in the absence of BMP-2, demonstrated an elevated OPN transcript level that was indistinguishable from the cells undergoing BMP-2 stimulation. The extent of OPN expression for MWCNT-PEG alone was in fact similar to that for PEG (+BMP-2) cells, confirming that the combination of nanotubes and PEG successfully guided cell differentiation toward bone formation. Interestingly, Briggs *et al.*,[32] observed that, while OPN is a gene up regulated during the initial mineralization phases of osteogenesis, other marker genes are critically up-regulated along with downstream programs for osteogenesis, as demonstrated by alkaline phosphatase activity and osteocalcin (OCN) expression. This effect was also observed when hMSCs were grown on polycarbonates copoly-

merized with 0−5% PEG. Therefore, we evaluated the influence of MWCNT-PEG on hMSC differentiation into osteogenic lineages by immunofluorescent staining of two common protein markers: CD44 for hMSCs and OCN for osteoblasts (Figure 5b−g). This investigation was performed after two weeks of incubation of hMSCs onto different substrates in the presence of osteogenic media. The immunofluorescence results clearly showed that cells growing on plain (Figure 5b) and only PEG-coated (Figure 5d) coverslips bound to the fluorescent antibody specific for CD44 expression, confirming the fact that hMSCs maintained significant features of "stemness" character (*i.e.*, lack of complete differentiation into osteogenic lineage). At the same time, these cells did not immunostain for OCN (Figure 5e and g) because they were not differentiated into osteoblast-like cells. Conversely, MWCNT-PEG samples did not express CD44 (Figure 5c), and instead they showed high fluorescence in correspondence of OCN immunostaining (Figure 5f), confirming a successful differentiation of hMSCs into osteoblasts even in absence of BMP-2. Moreover, since OCN is normally expressed after 21 days of *in vitro* osteogenesis of MSCs,[33] we theorized that MWCNT-PEG samples acted as a biochemical enhancer, accelerating the process of hMSCs differentiation into osteocyte phenotype. Such attributes may help to strengthen the bone structure and the eventual implants, *e.g.*, the area of defect could be quickly covered and bridged to surrounding bone by the thin film of nanotubes, which are strong enough to support and anchor the initial monolayer of cells over the whole period, from proliferation to differentiation, for the deposition of new bone. Indeed, numerous preclinical studies have shown that BMPs play a critical role in bone healing by stimulating the differentiation of mesenchymal cells to an osteogenic lineage.[34] Similarly Rawadi *et al.*[35] have reported the control of osteogenic induction and mineralization by BMP-2 in pluripotent mesenchymal cell lines C3H10T1/2, C2C12, and ST2 and in the osteoblast cell line MC3T3-E1. In our case, hMSCs were cultured in osteogenic medium with and without BMP-2. An additional sample consisted of BMP-2 covalently attached to MWCNT-COOH *via* carbodiimide chemistry (Scheme S1, Supporting Information).[36] Due to the coating procedures that require heating the coverslips at 160 °C (which would have hampered the activity of any protein, including BMP-2), we used the coverslips already coated with MWCNT-COOH for the subsequent covalent immobilization of BMP-2. After repeated washes to remove unspecific adsorption of inducer, the amount of BMP-2 covalently attached onto the MWCNT-COOH coating was analyzed by bovine carbonic anhydrase (BCA) protein assay using a previously prepared BMP-2 standard curve, and it was found to be 70 ng. This was comparable to the amount of BMP-2 (75 ng/well) added to the osteogenic media in case of osteoinduction experiments with hMSCs. Post confluence (12−14 days), cells cultured on different substrates [*i.e.*, (a) plain coverslips with and without BMP-2; (b) PEG alone; (c) MWCNT-PEG with and without BMP-2; and (d) MWCNT-COOH with BMP-2 covalently bound] were subjected to alizarin red quantification which, by staining calcium depositions as part of matrix mineralization, represents a functional proof of the terminal differentiation into osteocyte phenotype (Figure 5h).

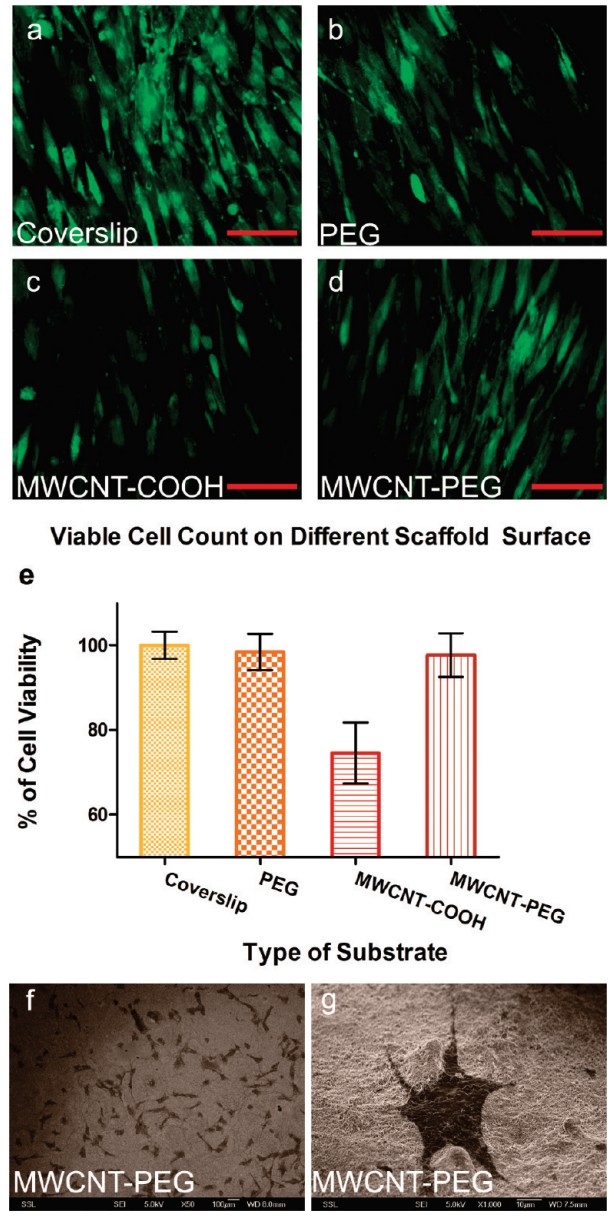

Figure 4. Cells growing on: (a) normal coverslip; (b) PEG-coated coverslip; (c) MWCNT-COOH-coated coverslip; (d) MWCNT-PEG-coated coverslips. Scale bars are 100 μm. (e) Graph showing percentage of cell viability of different substrates for hMSCs. (f and g) SEM images of hMSCs growing in normal medium on MWCNT-PEG-coated coverslips at day four of incubation. (f) Large field of view showing growth of lots of cells. Scale bar is 100 μm. (g) Small field of view showing a single cell. Scale bar is 10 μm.

Figure 5h shows that hMSCs grown on uncoated or PEG-only coated coverslips were not able to form calcium deposits, suggesting that osteogenic medium or PEG alone were not sufficient to induce proper differen-

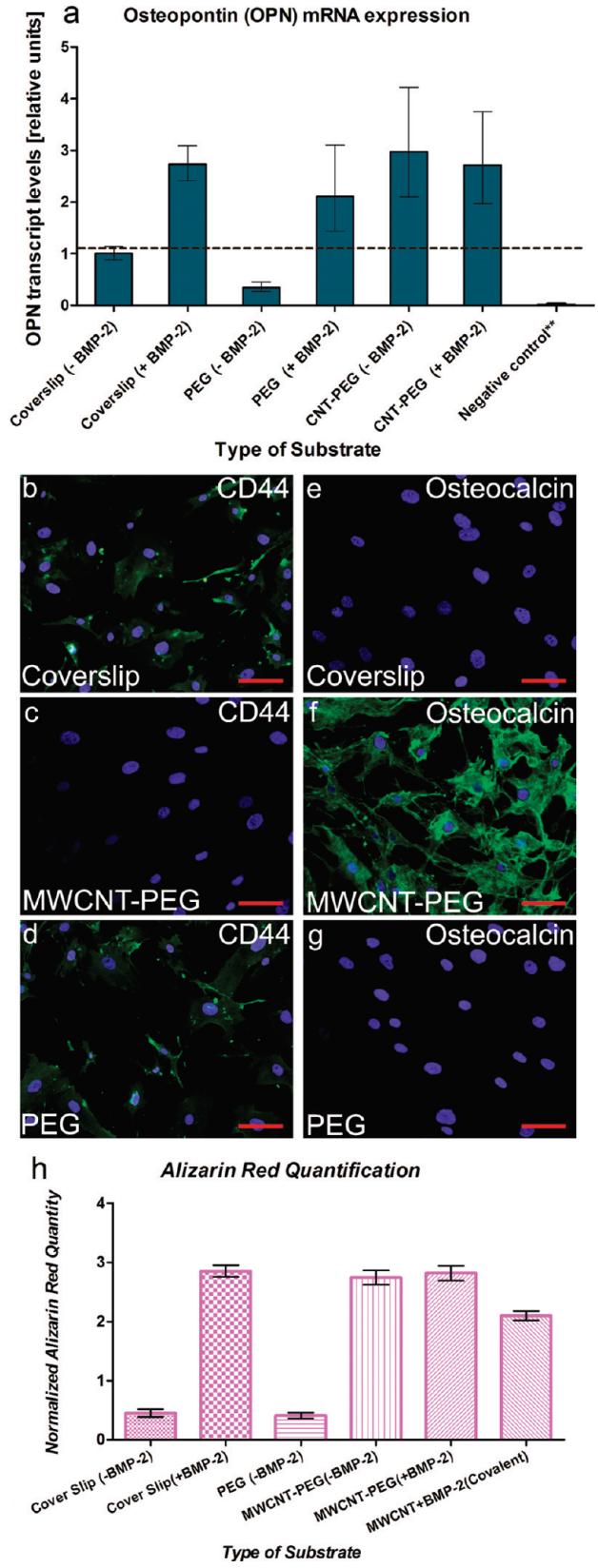

Figure 5. (a) qPCR analysis of relative expression levels of OPN for hMSCs cultured on different types of substrates and osteoinduced with osteogenic media with or without BMP-2 for 14 days. **Negative control consists of a coverslip without BMP-2 and without induction with osteogenic media. (b−g) Immunofluorescence image of cells subjected to osteoinduction without BMP-2. Cells growing on (b, e) plain coverslips showing the presence of CD44 and absence of OCN; (c, f) MWCNT-PEG-coated coverslips showing the absence of CD44 and presence of OCN; (d, g) only PEG-coated coverslips showing the presence of CD44 and absence of OCN. Scale bars are 100 μm. (h) Graph showing normalized alizarin red quantity in cells growing on different scaffold surfaces with or without BMP-2.

tiation of hMSCs into osteoblasts. Notably, although calcium can be deposited on some scaffolds, we did not observe any nonspecific staining from CNTs alone (without cells) based on alizarin red staining. Conversely, all the substrates with hMSCs treated with 70−75 ng/well of BMP-2 clearly showed abundant calcium deposition as indicated by a high normalized alizarin red quantity. Only the sample of MWCNT-COOH covalently bound to BMP-2 presented fewer calcium deposits, most probably due to a less uniform coating with MWCNT-COOH or to a partial denaturation of BMP-2 immobilized onto CNTs. With regards to this last aspect, it had already been demonstrated that immobilization of enzymes and proteins onto substrates sometimes affects their secondary structures and often decreases their activity.[37] Interestingly, both BMP-2 treated substrates and MWNT-PEG-coated (without BMP-2) coverslips showed comparable ($p > 0.05$) cell differentiation into bone cells. In other words, the uniform coating of MWCNT-PEG provided a suitable microenvironment for hMSCs proliferation and differentiation even in the absence of the standard biochemical inducer.

Altogether, MWCNT-PEG successfully transformed hMSC into bone-like cells even in the absence of any additional growth factor, as evidenced by multiple independent criteria at the transcript (*e.g.* OPN), protein (*e.g.*, OCN), and functional (*e.g.*, calcium deposition) levels.

CONCLUSIONS

It is widely known that extracellular matrix can exert highly complex biochemical effects in a similar way that growth factors can (*e.g.*, BMP-2),[38] resulting in dramatic changes to cell phenotypes. This study clearly illustrates that, by subjecting mesenchymal stem cells to an appropriately selected biomaterial, it is possible to propel the cells to differentiate into a targeted tissue type like osteoblasts. As this finding presents the next challenge of understanding the mechanistic basis for the differentiating pressure of MWCNT-PEG, it also underlies the promise of the ability that such material can differentiate into other tissue types (such as chondrocytes and myocytes) through subtle modification of the matrix and induction with specific media. Taken together, these results suggest a promising role for functionalized CNTs as reinforcing agents due to their high mechanical strength as well as their use as biocompatible scaffolds for applications in tissue engineering and bone repair.

MATERIALS AND METHODS

Functionalization of MWCNTs and Characterization. Ultrapure MWCNTs were functionalized following the procedure reported elsewhere[18] and illustrated in Scheme S1, Supporting Information. The extent of oxidation of MWCNTs, loading with PEG and dispersibility were determined by transmission electron microscopy (TEM), TGA, and dispersibility study, respectively (Supporting Information). While TEM was done using JEOL JEM 2010F HR-TEM (200KV Field Emission Gun), TGA data were recorded on a TA Instruments-SDT 2960 Simultaneous DTA-TGA (differential thermal/thermogravimetric analyzer), with a heating rate of 5 °C/min in air.

Coating of Coverslips and Their Characterization. Lyophilized samples of PEG-functionalized (MWCNT-PEG) and oxidized nanotubes (MWCNT-COOH), along with only PEG samples, were individually sonicated in Milli-Q water (produced using Millipore's Synergy water purification system with cartridge Simpak2) to obtain a 10 mg/mL suspension. The suspension was sprayed with an airbrush (Badger 100LG model) onto round glass coverslips (12 mm diameter, Electron Microscopy Sciences), which had been previously heated up to 160 °C to allow the fabrication of uniform films[11] (Figure S2, Supporting Information). Coated coverslips were allowed to dry in air and were used for cell culture after sterilization with UV irradiation overnight.

Some of the sterile MWCNT-COOH-coated coverslips were subjected to covalent attachment of the osteogenic inducer (bone morphogenetic protein or BMP-2), following the procedure mentioned elsewhere.[36] The amount of BMP-2 covalently immobilized onto MWCNT-COOH was determined by BCA protein assay (Pierce, Thermo Scientific), as mentioned in Supporting Information (paragraph 3d).

Optical pictures (Figure S3, Supporting Information) of coverslips coated with f-CNTs were taken to visualize any cracks in the coating visible under microscope (Nikon AZ-100). Similarly, AFM (Veeco dimension 3100, United States) was done to determine the roughness of coverslips coated with different f-CNTs. The scanning was done in tapping mode using a silicon nitride probe. The roughness was calculated in terms of the average deviation (three images for each sample) from the mean plain of surface. Root-mean square (rms) values and peak-to-peak ratios were also calculated to compare the roughness between different surfaces. AFM images of the samples were obtained by spraying the dispersions of f-MWCNTs (10 mg/mL) with an airbrush onto round coverslips (12 mm in diameter) heated to 160 °C.

Stem Cell Growth and Culture. The hMSCs of passage 1 were obtained courtesy of Dr. Rachel Ee of the Department of Pharmacy, National University of Singapore. The hMSCs were cultured in T75 culture flasks using Dulbecco's modified Eagle's medium (DMEM) prepared in Milli-Q water and added with essential ingredients (paragraph four in Supporting Information). The medium was refreshed every 3−4 days until the cells reached 80−90% confluence (12−14 days). Trypan blue dye exclusion assay was used to count viable cells for all experimental purpose.

Cytotoxicity Assays. To determine the cytotoxicity of ultrapure MWCNTs toward hMSCs, MTT and CyQUANT (Invitrogen) assays were performed according to the known procedures.[39,40]

Scanning Electron Microscopy. Cells (hMSCs) growing on MWCNT-PEG-coated coverslips were subjected to critical point drying[41] (BAL-TEC CPD 030) and dried for about 1 h. The pressure was released slowly after drying to avoid disturbing the coating on the coverslips. Finally cells on these MWCNT-PEG-coated coverslips were observed under field-emission scanning electron microscope (SEM) (JEOL JSM-6701F, Tokyo, Japan). The growth of hMSCs on MWCNT-COOH-coated coverslips could not be visualized by SEM as the coating was unstable during the process of critical point drying.

Fluorescence Microscopy. Coverslips coated with different substrates (MWCNT-COOH, MWCNT-PEG, and only PEG) along with uncoated (used as control) coverslips were put individually into wells of a 24 well plate (Greiner bio-one, Germany). The hMSCs were seeded (5000 cells/well) onto these wells and cultured as mentioned above. Post confluence, the medium was aspirated out of the wells, and all the coverslips having cells growing on them were transferred into a new 24 well plate. Cells in each cov-

erslip were washed carefully with 1 mL PBS for three times. Further 1 mL of PBS was added to each well followed by 5 μL of calcein AM (1 mM). The well plates were incubated for 30 min at room temperature in the dark. Finally all the coverslips were washed 3−4 times with PBS and were inverted onto glass slides mounted with 70% glycerol and visualized under fluorescence microscope (Nikon AZ-100 multipurpose microscope).

Calcein AM Cell Viability Assay. Similar procedure as mentioned above was followed with respect to staining of cells with calcein acetoxymethyl ester (AM). After washing all the coverslips 3−4 times with PBS, 1 mL of PBS was left on each well along with the wells having no cells as control. Fluorescence signal pertaining to excitation wavelength of 490 nm and emission wavelength of 520 nm was read using a microwell plate reader (Infinite 200). The number of viable cells was obtained for all the coverslips by comparing the fluorescence signals with a previously prepared calcein AM cell viability standard curve obtained using a known number of viable cells (2000−20 000) and utilizing the same procedure.

Osteogenic Induction and Differentiation. The osteogenic medium was prepared following known procedure[42] (Table S2, Supporting Information). The hMSCs at 5000 cells per well were seeded into a 24 well plate having both uncoated and MWCNT-coated coverslips. The well plate was left overnight inside the incubator at 37 °C for cells to adhere to the surface of tissue culture plates. After 24 h, osteogenesis was induced by replacing original medium in selected wells with osteogenic medium. BMP-2 (150 ng/mL) was added to osteogenic medium depending upon the purpose of the experiments. The osteogenic medium was replaced every 3 days until confluence (12−14 days) was reached. Osteoinduced cells were compared with noninduced cells on both uncoated and coated coverslips. Post confluence alizarin red quantification, immunofluorescence, and qPCR were performed on the cell samples.

Alizarin Red Quantification. Alizarin red quantification was performed to assess ECM mineralization after 14 days in osteogenic media with or without BMP-2. This was done by fixing cells with 100% ethanol for 15 min and then staining with 0.2% alizarin red solution with a pH between 6.36 and 6.4 at room temperature for 1 h. After 1 h, unbound alizarin red was aspirated, and bound alizarin red was quantified using 20% methanol (Tedia) and 10% acetic acid in water. After 15 min, the methanolic mixture for each sample was transferred to a 96 well plate (200 μL/well) and performed in triplicates. The quantity of alizarin red was read on the microplate reader at 450 nm and normalized to protein content using BCA protein assay (Pierce, Thermo Scientific).[33]

Immunofluorescence. Osteoinduction without BMP-2 was done for hMSCs growing on coverslips coated with different substrates (plain coverslips, coverslips coated with MWCNT-PEG and PEG alone), according to the procedure already mentioned before.

Post confluence, cells growing on coverslips were taken out from the wells and put into a newly marked 24 well plate. The cells on all the coverslips were fixed by treating with ice cold 50%/50% methanol/acetone. After 5 min, methanol/acetone solution was removed, and the coverslips were left open inside the laminar hood to be air-dried. After the coverslips were completely dried, the fixed cells were treated with 10% FBS in PBS (blocking agent) for 20 min. The blocking agent was aspirated, and 5 μL of different primary antibodies to cellular markers (CD44 for hMSCs and OCN for osteoblasts) were put onto different coverslips coated with each type of substrates (including plain coverslips used as a control) and incubated at room temperature. After 1 h, the cells on the coverslips were extensively washed with Milli-Q water for 5 min and then rinsed in PBS for 5 min. After that, 100 μL of diluted (1/100) secondary antibody (goat antimouse antibody) conjugated with a fluorescent dye (FITC) was added onto each coverslip (both coated and uncoated) and incubated at room temperature. After 30 min the coverslips having cells were washed with Milli-Q water and were inverted onto glass slides mounted with Vectashield with the fluorescent dye 4′,6-diamidino-2-phenylindole (DAPI, H 1200, Vector laboratories) and visualized under fluorescence microscope (Nikon AZ-100 multipurpose microscope). The pictures were taken separately at the same positions using both green fluorescent protein (GFP) and DAPI filter to capture both the fluorescence due to FITC conjugated secondary antibody staining the marker proteins and to DAPI staining the nucleus of each cell. Subsequently, images were merged using Nikon elements BR 3.1 image processing software.

Quantitative RT-PCR. Approximately 1 million cells from each BMP-2-treated and control experiment were harvested for RNA isolation using mirVana miRNA isolation kit (Ambion, Austin, TX), according to manufacturer's instructions. Total RNA was quantified, and the quality was ascertained (OD260/280 within 1.9−2.1) using NanoDrop (Thermo, Wilmington, DE). cDNAs of respective samples were synthesized from 0.3−1 μg of total RNA using SuperScript III reverse transcriptase (Invitrogen, Carlsbad, CA), according to manufacturer's instructions. Quantitative real-time-PCR was performed using Applied Biosystems 7500 Fast Real-Time PCR System with Fast SYBR Green master mix and primers for OPN (NM_001040058; F: 5′-ACG CCG ACC AAG GAA AAC TC-3′; R: 5′-GTC CAT AAA CCA CAC TAT CAC CTC G-3′). 18S RNA (NR_003286; F: 5′-CGG CTT AAT TTG ACT CAA CAC G-3′; R: 5′-TTA GCA TGC CAG AGT CTC GTT C-3′) were quantified as housekeeping control. The thermal cycling condition comprised an initial denaturation at 95 °C (20 s), followed by 40 cycles at 95 °C (3 s) and 60 °C (30 s). Melting curves were generated at the end of 40 cycles to verify the purity of the PCR product. The samples were prepared in triplicates with 4 μL of 10-fold-prediluted cDNA. Data were obtained as average C_T values and normalized against housekeeping control as ΔC_T. Expression changes in OPN transcripts in various samples were measured as fold change with respect to cells grown on coverslip in the absence of BMP-2 stimulation using $2^{\Delta\Delta C_T}$ ($\Delta\Delta C_T = \Delta C_T$ of test sample $- \Delta C_T$ of control cells) (Table S3, Supporting Information).

Statistical Analysis of the Data. All the data from cell viability assays, alizarin red quantification, and qPCR were subjected to student *t*-test to calculate *p*-value. If the *p*-value was found to be less than the threshold (0.05) chosen for statistical significance, then the null hypothesis (which states that the two groups do not differ) was rejected in favor of an alternative hypothesis, which indicates that the groups do differ significantly.

Acknowledgment. This research has been supported by the National University of Singapore, Department of Pharmacy (FRC grant R-148-000-129-112), A-STAR (grant SERC R-148-001-435-305) and by MOE of Singapore (grant MOE2009-T2-2-011, R-398-000-068-112). We thank T. Arockiadoss and S. Ramaprabhu from the Indian Institute of Technology (India) for the samples of ultrapure nanotubes and also R. Ee Pui-Lai for assistance on cell work and the Nikon Imaging Centre, Singapore Bioimaging Consortium, for providing technical assistance and microscope facilities.

Supporting Information Available: Materials and methods involving synthesis and characterization of the functionalized MWCNTs, together with cell culture and qPCR. This material is available free of charge *via* the Internet at http://pubs.acs.org.

REFERENCES AND NOTES

1. Langer, R.; Vacanti, J. P. Tissue Engineering. *Science* **1993**, *260*, 920–6.
2. Freed, L. E.; Vunjak-Novakovic, G. *Tissue Engineering Bioreactors*; 2nd ed.; Academic Press: San Diego, CA, 2000; p 143−156.
3. Dyke, C. A.; Tour, J. M. Unbundled and Highly Functionalized Carbon Nanotubes From Aqueous Reactions. *Nano Lett.* **2003**, *3*, 1215–1218.
4. Holzinger, M.; Vostrowsky, O.; Hirsch, A.; Hennrich, F.; Kappes, M.; Weiss, R.; Jellen, F. Sidewall Functionalization of Carbon Nanotubes This work was supported by the European Union under the 5th Framework Research Training Network 1999, HPRNT 1999−00011 FUNCARS. *Angew. Chem., Int. Ed. Engl.* **2001**, *40*, 4002–4005.
5. Sittinger, M.; Bujia, J.; Rotter, N.; Reitzel, D.; Minuth, W. W.; Burmester, G. R. Tissue Engineering and Autologous Transplant Formation: Practical Approaches with

Resorbable Biomaterials and New Cell Culture Techniques. *Biomaterials* **1996**, *17* (3), 237–42.
6. Vacanti, J. P.; Langer, R. Tissue Engineering: The Design and Fabrication of Living Replacement Devices for Surgical Reconstruction and Transplantation. *Lancet* **1999**, *354* (1), SI32−4.
7. Khademhosseini, A.; Vacanti, J. P.; Langer, R. Progress in Tissue Engineering. *Sci. Am.* **2009**, *300*, 64–71.
8. Zippel, N.; Schulze, M.; Tobiasch, E. Biomaterials and Mesenchymal Stem Cells for Regenerative Medicine. *Recent Pat. Biotechnol.* **2010**, *4*, 1–22.
9. Murphy, R.; Coleman, J. N.; Cadek, M.; McCarthy, B.; Bent, M.; Drury, A.; Barklie, R. C.; Blau, W. J. High-Yield, Nondestructive Purification and Quantification Method for Multiwalled Carbon Nanotubes. *J. Phys. Chem. B* **2002**, *106*, 3087–3091.
10. Hu, H.; Ni, Y. C.; Montana, V.; Haddon, R. C.; Parpura, V. Chemically Functionalized Carbon Nanotubes as Substrates for Neuronal Growth. *Nano Lett.* **2004**, *4*, 507–511.
11. Malarkey, E. B.; Fisher, K. A.; Bekyarova, E.; Liu, W.; Haddon, R. C.; Parpura, V. Conductive Single-Walled Carbon Nanotube Substrates Modulate Neuronal Growth. *Nano Lett.* **2009**, *9*, 264–268.
12. Mazzatenta, A.; Giugliano, M.; Campidelli, S.; Gambazzi, L.; Businaro, L.; Markram, H.; Prato, M.; Ballerini, L. Interfacing Neurons with Carbon Nanotubes: Electrical Signal Transfer and Synaptic Stimulation in Cultured Brain Circuits. *J. Neurosci.* **2007**, *27*, 6931–6936.
13. Park, H.; Cannizzaro, C.; Vunjak-Novakovic, G.; Langer, R.; Vacanti, C. A.; Farokhzad, O. C. Nanofabrication and Microfabrication of Functional Materials for Tissue Engineering. *Tissue Eng.* **2007**, *13*, 1867–77.
14. Park, J.; Bauer, S.; Schlegel, K. A.; Neukam, F. W.; von der Mark, K.; Schmuki, P. TiO2 Nanotube Surfaces: 15 nm--an Optimal Length Scale of Surface Topography for Cell Adhesion and Differentiation. *Small* **2009**, *5*, 666–71.
15. Engler, A. J.; Sen, S.; Sweeney, H. L.; Discher, D. E. Matrix Elasticity Directs Stem Cell Lineage Specification. *Cell* **2006**, *126*, 677–89.
16. Engler, A. J.; Sweeney, H. L.; Discher, D. E.; Schwarzbauer, J. E. Extracellular Matrix Elasticity Directs Stem Cell Differentiation. *J. Musculoskeletal Neuronal Interact.* **2007**, *7*, 335.
17. Dalby, M. J.; Gadegaard, N.; Tare, R.; Andar, A.; Riehle, M. O.; Herzyk, P.; Wilkinson, C. D.; Oreffo, R. O. The Control of Human Mesenchymal Cell Differentiation using Nanoscale Symmetry and Disorder. *Nat. Mater.* **2007**, *6*, 997–1003.
18. Zhao, B.; Hu, H.; Yu, A.; Perea, D.; Haddon, R. C. Synthesis and Characterization of Water Soluble Single-Walled Carbon Nanotube Graft Copolymers. *J. Am. Chem. Soc.* **2005**, *127*, 8197–203.
19. Jongpaiboonkit, L.; King, W. J.; Murphy, W. L. Screening for 3D Environments that Support Human Mesenchymal Stem Cell Viability using Hydrogel Arrays. *Tissue Eng., Part A* **2009**, *15*, 343–53.
20. Elisseeff, J.; Puleo, C.; Yang, F.; Sharma, B. Advances in Skeletal Tissue Engineering with Hydrogels. *Orthod Craniofac. Res.* **2005**, *8*, 150–61.
21. Bowers, K. T.; Keller, J. C.; Randolph, B. A.; Wick, D. G.; Michaels, C. M. Optimization of Surface Micromorphology for Enhanced Osteoblast Responses In Vitro. *Int. J. Oral Maxillofac. Implants* **1992**, *7*, 302–10.
22. Keller, J. C.; Collins, J. G.; Niederauer, G. G.; McGee, T. D. In Vitro Attachment of Osteoblast-like Cells to Osteoceramic Materials. *Dent. Mater.* **1997**, *13*, 62–8.
23. Gomi, K.; Davies, J. E. Guided Bone Tissue Elaboration by Osteogenic Cells In Vitro. *J Biomed Mater Res* **1993**, *27*, 429–31.
24. Curtis, A. S.; Wilkinson, C. D. Reactions of Cells to Topography. *J. Biomater. Sci., Polym. Ed.* **1998**, *9*, 1313–29.
25. Oh, S.; Brammer, K. S.; Li, Y. S. J.; Teng, D.; Engler, A. J.; Chien, S.; Jin, S. Stem Cell Fate Dictated Solely by Altered Nanotube Dimension. *Proc. Natl. Acad. Sci. U.S.A.* **2009**, *106*, 2130–2135.
26. Nayak, T. R.; Leow, P. C.; Ee, P. L. R.; Arockiadoss, T.; Ramaprabhu, S.; Pastorin, G. Crucial Parameters Responsible for Carbon Nanotubes Toxicity. *Curr. Nanosci.* **2010**, *6*, 141–154.
27. Bratosin, D.; Mitrofan, L.; Palii, C.; Estaquier, J.; Montreuil, J. Novel Fluorescence Assay using Calcein-AM for the Determination of Human Erythrocyte Viability and Aging. *Cytometry, Part A* **2005**, *66*, 78–84.
28. Dumortier, H.; Lacotte, S.; Pastorin, G.; Marega, R.; Wu, W.; Bonifazi, D.; Briand, J. P.; Prato, M.; Muller, S.; Bianco, A. Functionalized Carbon Nanotubes are Non-Cytotoxic and Preserve the Functionality of Primary Immune Cells. *Nano Lett.* **2006**, *6*, 1522–8.
29. Sayes, C. M.; Liang, F.; Hudson, J. L.; Mendez, J.; Guo, W.; Beach, J. M.; Moore, V. C.; Doyle, C. D.; West, J. L.; Billups, W. E.; et al. Functionalization Density Dependence of Single-Walled Carbon Nanotubes Cytotoxicity In Vitro. *Toxicol. Lett.* **2006**, *161*, 135–42.
30. Liu, D. D.; Yi, C. Q.; Zhang, D. W.; Zhang, J. C.; Yang, M. S. Inhibition of Proliferation and Differentiation of Mesenchymal Stern Cells by Carboxylated Carbon Nanotubes. *ACS Nano* **2010**, *4*, 2185–2195.
31. Liu, F.; Akiyama, Y.; Tai, S.; Maruyama, K.; Kawaguchi, Y.; Muramatsu, K.; Yamaguchi, K. Changes in the Expression of CD106, Osteogenic Genes, and Transcription Factors Involved in the Osteogenic Differentiation of Human Bone Marrow Mesenchymal Stem Cells. *J. Bone Miner. Metab.* **2008**, *26*, 312–20.
32. Briggs, T.; Treiser, M. D.; Holmes, P. F.; Kohn, J.; Moghe, P. V.; Arinzeh, T. L. Osteogenic Differentiation of Human Mesenchymal Stem Cells on Poly(ethylene glycol)-Variant Biomaterials. *J. Biomed. Mater. Res. A* **2009**, *91*, 975–84.
33. Tataria, M.; Quarto, N.; Longaker, M.; Sylvester, K. Absence of the p53 Tumor Suppressor Gene Promotes Osteogenesis in Mesenchymal Stem Cells. *J. Pediatr. Surg.* **2006**, *41*, 624–632.
34. Wang, E. A.; Israel, D. I.; Kelly, S.; Luxenberg, D. P. Bone Morphogenetic Protein-2 Causes Commitment and Differentiation in C3H10T1/2 and 3T3 Cells. *Growth Factors* **1993**, *9*, 57–71.
35. Rawadi, G.; Vayssiere, B.; Dunn, F.; Baron, R.; Roman-Roman, S. BMP-2 Controls Alkaline Phosphatase Expression and Osteoblast Mineralization by a Wnt Autocrine loop. *J. Bone Miner. Res.* **2003**, *18*, 1842–53.
36. Asuri, P.; Karajanagi, S. S.; Sellitto, E.; Kim, D. Y.; Kane, R. S.; Dordick, J. S. Water-Soluble Carbon Nanotube-Enzyme Conjugates as Functional Biocatalytic Formulations. *Biotechnol. Bioeng.* **2006**, *95*, 804–11.
37. Cang-Rong, J. T.; Pastorin, G. The Influence of Carbon Nanotubes on Enzyme Activity and Structure: Investigation of Different Immobilization Procedures Through Enzyme Kinetics and Circular Dichroism Studies. *Nanotechnology* **2009**, *20*, 255102.
38. Hidalgo-Bastida, L. A.; Cartmell, S. H. Mesenchymal Stem Cells, Osteoblasts and Extracellular Matrix Proteins: Enhancing Cell Adhesion and Differentiation for Bone Tissue Engineering. *Tissue Eng., Part B* **2010**, *16*, 405–12.
39. Mosmann, T. Rapid Colorimetric Assay for Cellular Growth and Survival: Application to Proliferation and Cytotoxicity Assays. *J. Immunol. Methods* **1983**, *65*, 55–63.
40. Blaheta, R. A.; Franz, M.; Auth, M. K.; Wenisch, H. J.; Markus, B. H. A Rapid Non-Radioactive Fluorescence Assay for the Measurement of Both Cell Number and Proliferation. *J. Immunol. Methods* **1991**, *142*, 199–206.
41. Minqin, R.; van Kan, J. A.; Bettiol, A. A.; Daina, L.; Gek, C. Y.; Huat, B. B.; Whitlow, H. J.; Osipowicz, T.; Watt, F. Nano-Imaging of Single Cells using STIM. *Nucl. Instrum. Methods Phys. Res., Sect. B* **2007**, *260*, 124–129.
42. Im, G. I.; Shin, Y. W.; Lee, K. B. Do adipose tissue-derived mesenchymal stem cells have the same osteogenic and chondrogenic potential as bone marrow-derived cells. *Osteoarthritis Cartilage* **2005**, *13* (10), 845–853.